

HIGH TEMPERATURE THERMAL STORAGE FOR SOLAR GAS TURBINES USING ENCAPSULATED PHASE CHANGE MATERIALS

Peter Klein¹, Thomas Roos², and John Sheer³

¹ BSc (Eng), School of Mechanical Industrial and Aeronautical Engineering, University of the Witwatersrand, Johannesburg 2000, South Africa, pklein@csir.co.za

² M. Eng. (Mech), Principal Research Engineer, Council for Scientific and Industrial Research

³ PhD, Visiting Professor, School of Mechanical Industrial and Aeronautical Engineering, University of the Witwatersrand

Abstract

The development of high temperature thermal storage systems is required to increase the solar share of solar-hybrid gas turbine cycles. This paper proposes a pressurised packed bed of Encapsulated Phase Change Materials (EPCM) as a thermal storage system for a gas microturbine. Sodium sulphate, with a melting temperature of 884 °C, was identified as a suitable low cost PCM and both macro and micro-encapsulation techniques were analysed. A numerical model of the EPCM concept was developed and used to compare the storage system with sensible heat storage in ceramic media. The results show that the discharge time of EPCM storage is comparable (<10 % improvement) with a packed bed of alumina particles, while the total storage mass is reduced by up to 31 %. The decrease in ceramic material costs must be higher than the encapsulation costs for this storage technology to be viable. A preliminary cost analysis is provided for the maximum allowable encapsulating costs.

Keywords: Thermal energy storage; phase change material (PCM); packed bed; gas turbine.

1. Introduction

South Africa's world class solar resource is set against a backdrop where 27 % of the population, mainly those in rural areas, do not have access to electricity [1]. The development of a solar-hybrid gas turbine cycle offers new opportunities for off the grid solar power generation. Recuperated gas microturbines (100 kW_e to 350 kW_e) are suited to solar thermal applications as they possess good cycle efficiencies (~30 %), require no cooling water and are readily hybridisable with fossil fuels. The overall efficiency of these cycles can be further increased by utilising the waste heat generated from the turbine to drive a non electric bottoming cycle such as an absorption chiller or a multi effect desalination unit.

In order to increase the solar share of Solar Gas Turbine (SGT) cycles, further research into high temperature thermal storage systems (≥900 °C) is required. Amsbeck *et al.* [2] proposed a pressurised packed bed concept as a direct thermal storage system for a solarised gas microturbine (Turbec T100). Packed beds have the potential to provide efficient thermal storage systems when the working fluid is air as they have a large surface area for heat exchange and show high rates of heat transfer.

A diagram of a recuperated SGT cycle with pressurised thermal storage is presented in Fig. 1. In order to solarise a gas microturbine certain modifications are made to the standard recuperated Brayton cycle. Concentrated solar energy is used to heat the turbine air stream in a pressurised air receiver located between the recuperator and combustion chamber. The series connection of the receiver and combustor allows for hybridisation of solar energy with conventional fossil fuels. The packed bed thermal storage system is connected in parallel with the receiver. During periods of excess energy supply a portion of the mass flow is re-circulated through the receiver and packed bed using a blower. Thus the mass flow rate through the receiver is higher than through the turbine in order to maintain a uniform receiver outlet temperature [3]. When there is a deficit in solar energy supply, due to weather conditions or the diurnal cycle of the sun, a fraction of the air mass flow is diverted through the packed bed to withdraw stored thermal energy.

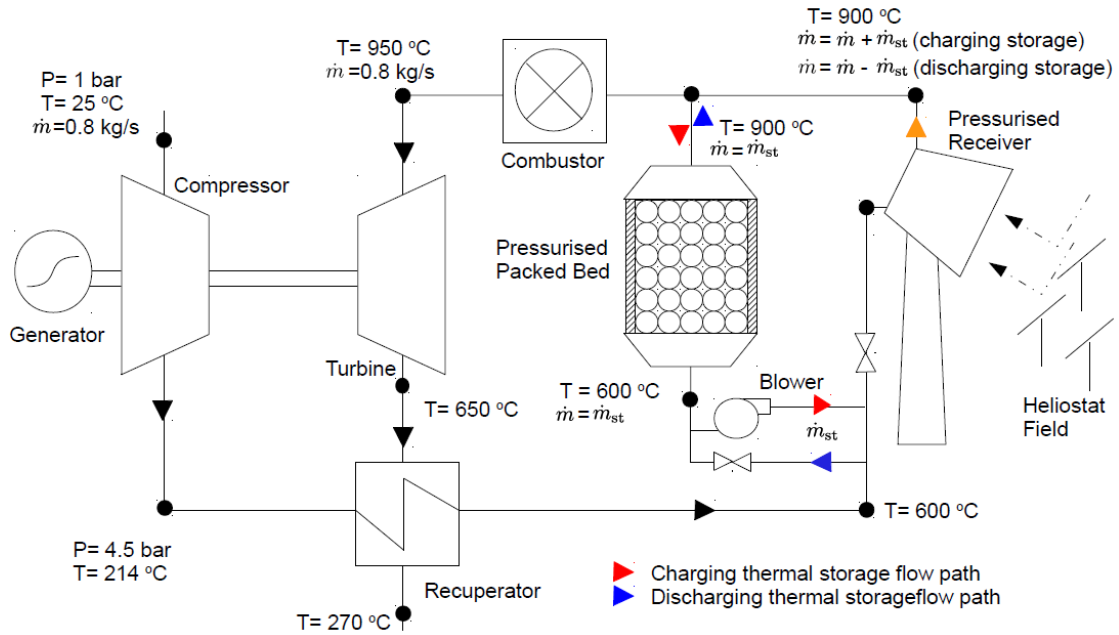


Fig. 1. Solarised Turbec 100 kW_e gas microturbine cycle with thermal storage (modified from [3]).

2. Latent Heat Thermal Storage

2.1. Background

Thermal energy can be stored in sensible heat, latent heat or thermochemical energy storage systems. Too *et al.* [4] reviewed several high temperature storage systems and stated that sensible heat storage in ceramic media is most likely to be implemented into SGT cycles in the near term. Sensible heat storage in packed beds involves a random packing of ceramic pebbles/particles in an insulated container. The temperature change of the solid during charging/discharging is used to store/release thermal energy. The primary disadvantage of sensible heat storage is the low energy storage density. Thus these systems require a large ceramic storage mass that is expensive and energy-intensive to manufacture. Due to the difficulties associated with piping hot pressurised air, the proposed storage system will be located in the receiver tower, near to the turbine. A large storage mass would therefore require increased structural support required in the tower.

Latent heat thermal storage systems are based on the melting and solidification of a Phase Change Material (PCM). These storage designs offer higher energy storage densities than sensible heat systems. The storage cost can also be reduced when readily available, low cost, PCMs are utilised. Suitable high temperature inorganic PCMs include alkali-metal and alkaline-earth-metal fluoride, chloride, carbonate and sulphate salts. Unfortunately the thermal conductivity of these salts in molten state is low (<1 W/mK) and the rate of heat transfer during cooling is limited by the solidification of the PCM on the heat transfer surfaces. The poor heat transfer through the salt can be mitigated by utilising a packed bed arrangement consisting of encapsulated Phase Change Materials (EPCMs). This method involves the retention of the PCM within an inert shell or matrix material. The high surface area of the packed bed increases the rate of heat transfer in the latent heat storage system. The EPCM particles also provide a self supporting structure to retain the molten PCM, thus eliminating corrosion issues with a metal packed bed wall. EPCM particles are not limited to inorganic salts. Metallic PCMs can also be considered, although at a higher cost.

2.2. Micro-encapsulation of PCM

Micro-encapsulation technology involves the immobilisation of a PCM within the porous structure of a ceramic material. When the PCM is melted it is held within the ceramic pores by capillary effect. The PCM to ceramic weight ratio of this composite material is typically varied between 20-50 % [5]. Thus this system represents a combined sensible-latent heat storage concept. The salt-ceramic material can be prepared by

either cold pressing and sintering a homogenized mixture of the ceramic and PCM powders, or by infusing a pre-sintered porous ceramic structure with the molten PCM.

Micro-encapsulation of PCMs was first developed by the Institute of Gas Technology in the 1980's [6]. In 1988 the German Aerospace Centre (DLR), Didier Ceramics and Stuttgart University began a research programme to investigate composite salt-ceramic materials for thermal storage applications. $\text{Na}_2\text{SO}_4/\text{SiO}_2$ was manufactured using the cold pressing method and extensively tested with respect to thermal, chemical and mechanical stability. The results indicated that the composite material was stable after repeated thermal cycling above the melting point of the Na_2SO_4 . Thus the pore fraction of the matrix was large enough to allow for the expansion of the salt without cracking the ceramic [5].

The composite $\text{Na}_2\text{CO}_3\text{-BaCO}_3/\text{MgO}$ was studied at the Oak Ridge National Laboratory in the USA [7]. This material was also prepared by cold pressing and sintering. Although the material was mechanically stable, heat transfer testing showed that the molten salt could evaporate when subjected to high temperature gas flow. Although the overall loss of salt in the system was less than 1 %, there was redistribution of salt within the packed bed due to vaporization and condensation effects.

2.3. Macro-encapsulation of PCM

In the macro-encapsulation approach the PCM is retained within a hollow shell material. The shell can be preformed, filled with a molten PCM and sealed; or it can be formed by coating a solid PCM particle. Macro-encapsulation allows for a higher percentage of PCM in the system. Another advantage is that the PCM is never in direct contact with the gas stream, thus eliminating any evaporation problems. However, the manufacturing process is more difficult than for micro-encapsulation. Inorganic salts in particular undergo large changes in volume upon melting (up to 30 %). The internal capsule design must therefore include a void to allow for the expansion of the PCM.

Mathur *et al.* [8] developed a coating process to encapsulate NaNO_3 particles (10-15 mm) using an inorganic shell consisting of kaolin and Montmorillonite clay. The shell was designed to be porous to gasses and a void in the particles was created by burning off a sacrificial coating layer on the NaNO_3 . Goswami [9] investigated two methods for macro-encapsulation of NaCl particles. The first method involves the use of preformed ceramic shells that are filled with NaCl . The second method uses direct ceramic coating of NaCl particles. In both procedures the ceramic shell with NaCl core was subsequently metal plated using electroless and electrochemical deposition techniques.

3. Numerical Modelling

This research aims at benchmarking EPCMs against solid ceramic particles, for use as filler materials in a high temperature packed bed thermal storage system. The three types of particles that were analysed are presented in Fig. 2. In each simulation the cylindrical bed dimensions were constrained to an internal volume of 6 m^3 ($D=1.5 \text{ m}$). The bed was assumed to be at a uniform temperature of $900 \text{ }^\circ\text{C}$ prior to the discharging at a mass flow rate of 0.8 kg/s (4.5 bar pressure).

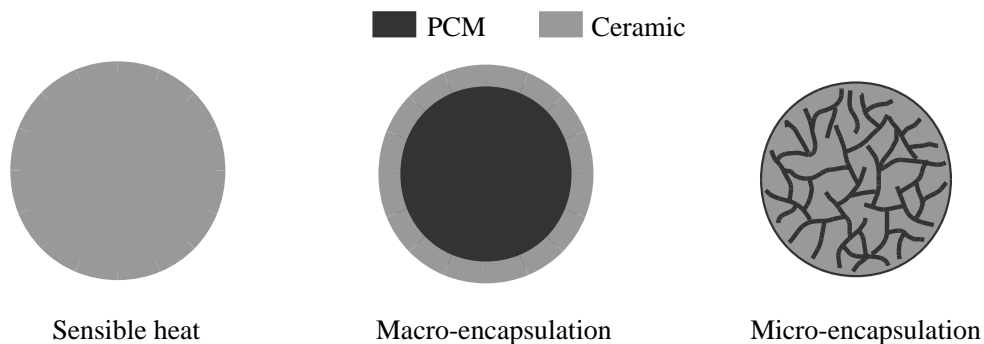


Fig. 2. Types of packed bed particles studied in present work.

3.1. Packed bed heat transfer model

The heat transfer within the packed bed was simulated using the Dispersion-Concentric (D-C) model of Wakao and Kaguei [10]. This model accounts for intraparticle temperature gradients by assuming a concentric temperature profile within a series of representative spherical particles. Energy is exchanged between the particle surfaces and the fluid by convection. The model assumes a perfectly insulated packed bed subjected to plug flow. Interparticle heat transfer via conduction and radiation is neglected. The governing energy equations for the fluid (Eq. 1) and solid phases (Eq. 2) were solved by orthogonal collocation on finite elements.

$$\varepsilon \rho_f c_f \left(\frac{\partial T_f}{\partial t} + U_x \frac{\partial T_f}{\partial x} \right) = h_p a_p (T_s|_{r=R} - T_f) + \frac{\partial}{\partial x} \left(\alpha_x \frac{\partial T_f}{\partial x} \right) \quad (1)$$

$$\rho_s c_{\text{eff}} \frac{\partial T_s}{\partial t} = \frac{1}{r^2} \frac{\partial}{\partial r} \left(r^2 k_{\text{eff}} \frac{\partial T_s}{\partial r} \right) \quad (2)$$

The simulation boundary conditions are presented in Fig. 3. The fluid phase boundary conditions represent the conditions at the inlet and exit of the packed bed. Discharging was initiated by applying a step change in the fluid inlet temperature from 900 °C to 600 °C. An adiabatic boundary condition was applied at the bed exit as no further heat transfer takes place with the solid particles. Convection heat transfer and symmetry boundary conditions were applied to the solid surfaces and centres respectively.

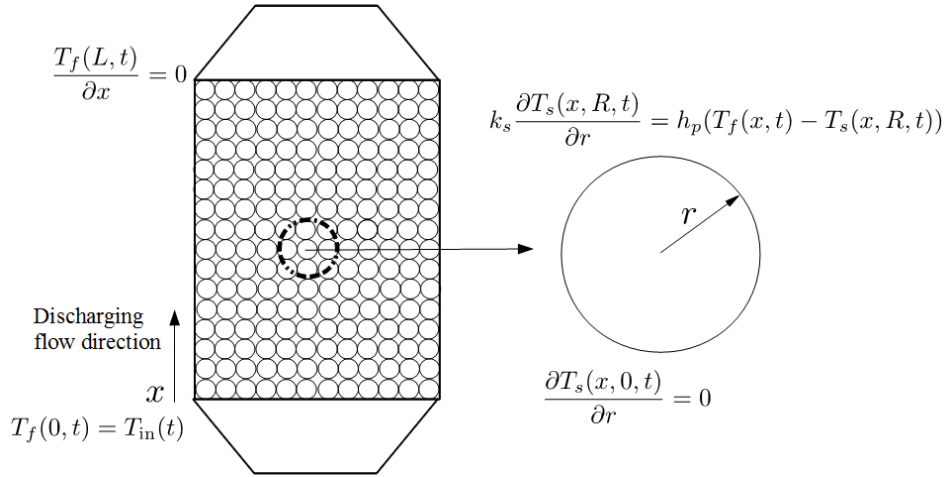


Fig. 3. Boundary conditions for D-C heat transfer model.

3.2. Phase change heat transfer model

The standard D-C model is based on solid conduction within each spherical particle. In order to account for the phase change within the EPCMs the ‘apparent heat capacity method’ [11] was used. This method requires the assumption that the PCM melts over a small temperature range ΔT_m and that there are no volumetric changes in the PCM during transformation. When the temperature of the PCM moves through the melting region the heat capacity is modified according to:

$$c_{\text{eff}} = c_s \quad \text{if} \quad T_s < T_m - \frac{\Delta T_m}{2} \quad (3)$$

$$c_{\text{eff}} = \frac{\Delta H_{fs}}{\Delta T_m} \quad \text{if} \quad T_m - \frac{\Delta T_m}{2} \leq T_s \leq T_m + \frac{\Delta T_m}{2} \quad (4)$$

$$c_{\text{eff}} = c_l \quad \text{if} \quad T_s > T_m + \frac{\Delta T_m}{2} \quad (5)$$

3.3. Validation of modelling

The D-C heat transfer model was validated against the experimental data of Klein *et al.* [3] for the case of sensible heat storage. The measured axial temperature profiles within the packed bed were compared to the D-C model with good accuracy, when the core flow velocity was reduced to account for wall channelling. The results are presented in Figure 4a). At present experimental data on conduction heat transfer within a high temperature PCM (Na_2SO_4) undergoing a phase change is not available. Therefore the ‘apparent heat capacity’ conduction model was validated against the analytical solution to the Stefan problem [12]. Figure 4b) shows that the numerical method can accurately reproduce the analytical solution.

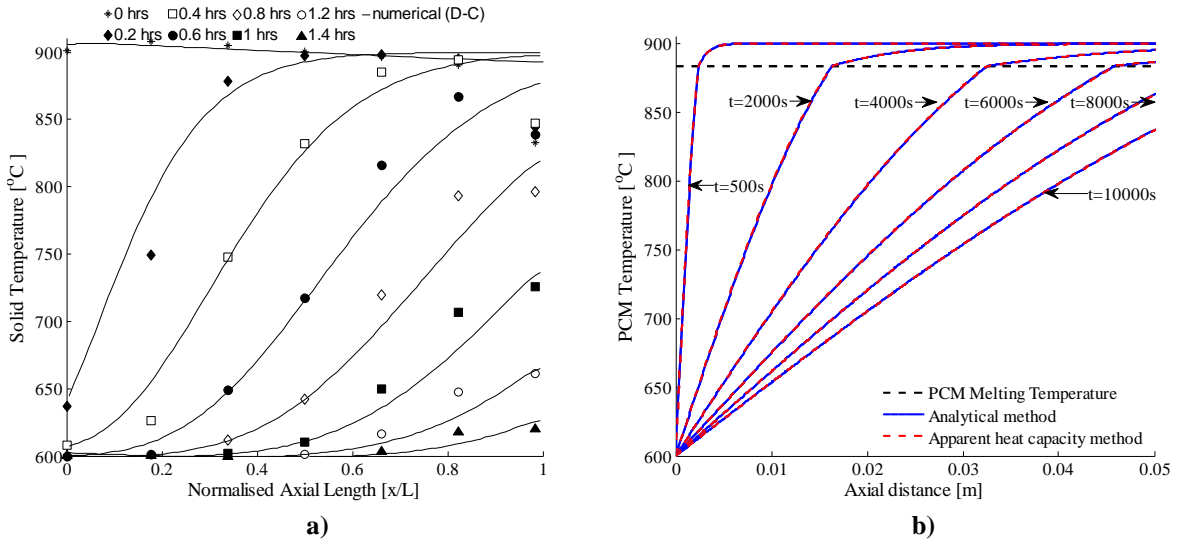


Fig. 4. Validation of numerical modelling; a) D-C model for sensible heat storage, b) Stefan problem for PCM conduction.

3.4. Ceramic and PCM storage materials

A broad survey of ceramic and PCM storage materials is outside the scope of this paper. The heat storage properties of a selection of materials are presented in Table 1. Alumina and fireclay were chosen for the sensible heat storage analysis. The high density of alumina (assumed to be sintered to 3600 kg/m^3) allows for a high volumetric heat capacity. However, the cost of pure alumina material can be high: the $1 \text{ MWh}_{\text{th}}$ alumina packed bed storage system installed at the TSA power tower cost more than $100 \text{ €/kWh}_{\text{th}}$. This is approximately 2-3 times the cost of a two-tank molten salt storage system. Fireclay based ceramics have a lower volumetric heat storage capacity than alumina but are available at a lower material cost.

The sodium salts Na_2SO_4 , Na_2CO_3 and NaCl were identified as potential low cost inorganic salts for EPCM thermal storage. Alumina was selected as the inert encapsulation material. For the macro-encapsulated pebbles a shell thickness of $0.05d_p$ was used. A 50:50 salt-to-alumina volume fraction was used for the micro-encapsulated particles. Simulations done in HSC Chemistry software indicated that Na_2CO_3 will react with alumina at high temperature. Therefore Na_2SO_4 was selected as the primary PCM for this analysis as it has a melting temperature close to 900 °C .

Table 1. Enthalpy change of storage materials between 600 °C and 900 °C

Material	T_m [°C]	H_{fs}^* [kJ/kg]	ΔH^* [kJ/kg]	$\Delta H/V^{**}$ [MJ/m ³]	Material	T_m [°C]	H_{fs}^* [kJ/kg]	ΔH^* [kJ/kg]	$\Delta H/V^{**}$ [MJ/m ³]
Al_2O_3	n/a	n/a	364	1312	Na_2CO_3	851	280	749	1620
Fireclay	n/a	n/a	345	759	NaCl	801	482	757	1132
Na_2SO_4	884	162	605	1170	Al	660	403	702	1452

* Enthalpy of fusion taken data taken from [13]

** Molten PCM density data taken from [14]

4. Results

4.1. Discharge time

In each simulation the storage was discharged until the exit air temperature dropped below 850 °C. As the volume of the packed bed was fixed, the efficiency of the different storage materials was determined by the length of time (t_d) that the outlet air temperature remained above 850 °C. These results are presented in Table 2.

For sensible heat storage the packed bed of alumina particles demonstrates a longer discharging time than the fireclay particles. This result is expected, as the sensible heat storage capacity of a material is directly related to its mass. The inventory mass of the fireclay is 39 % lower than the alumina mass for an equal volume packed bed. Therefore alumina was chosen for comparison against the EPCMs as it has a higher volumetric heat capacity.

The simulations indicate that macro and micro-encapsulated Na_2SO_4 particles provide a marginal (<10%) increase in discharge time when compared to solid alumina particles. The true benefit of the encapsulated particles therefore lies in the decrease in alumina mass within the packed bed. This is advantageous as the cost of the alumina ceramic is an order of magnitude more expensive than the Na_2SO_4 . The reduction in total bed mass will also decrease the cost of structural support required for the storage in the receiver tower. The mass of the alumina and Na_2SO_4 associated with each encapsulation technique is given in Table 2. Compared to solid alumina particles, the macro-encapsulated particles achieve a 73 % reduction in alumina mass and 31 % reduction in total bed mass (including alumina and PCM mass). The micro-encapsulated particles have a lower weight percentage of Na_2SO_4 and therefore achieve a 50 % reduction in alumina mass and 21 % reduction in total bed mass.

Table 2. Discharge time and associated mass of packed bed filler materials

Material	Mass [tonnes]	Al_2O_3 Mass [tonnes]	Na_2SO_4 Mass [tonnes]	$t_d(d_p=20 \text{ mm})$ [hrs]	$t_d(d_p=40 \text{ mm})$ [hrs]
Al_2O_3	13.0	13.0	0	4.10	3.73
Fireclay	7.9	n/a	0	2.50	2.31
Na_2SO_4 (Macro)	8.9	3.5	5.4	4.32	4.07
Na_2SO_4 (Micro)	10.2	6.5	3.7	4.29	3.99

4.2. Thermocline graphs

The transient temperature profiles within the different EPCM packed beds are presented in Figs. 5-7. These graphs allow for the heat transfer within the EPCM packed bed configurations to be analysed. The fluid and solid phase temperatures are plotted against time from five axial locations in the bed. The effect of the Na_2SO_4 phase change is to cause a plateau in the temperature profiles at 884 °C.

Figure 5 shows that there is a large temperature difference between the centre and surface of the 40 mm diameter macro-encapsulated particles. This is due to the poor thermal conductivity of the molten Na_2SO_4 , which limits the rate of intraparticle heat transfer. At present natural convection effects within the macro-encapsulated particles have not been taken into account. These will increase the intraparticle heat transfer rate for large particles. As shown in Fig. 6 the temperature difference between the particle surface and centre is reduced for the smaller 20 mm diameter particle size. This is due to the decrease in the conduction length across the particle. Another benefit of the smaller particle size is the higher surface area for heat exchange with the air. This causes a steeper thermocline (axial temperature front) to develop that increases the discharge time. The disadvantages of the smaller encapsulated particles include a higher pressure drop and an increase in the number of particles that must be manufactured. The encapsulation process will have a cost per particle that must be encapsulated. As the volume of each particle is a function of d_p^3 , halving the particle diameter increases the number of particles that are required by a factor of 8. Therefore the particle diameter should be optimised from a manufacturing cost and heat transfer perspective.

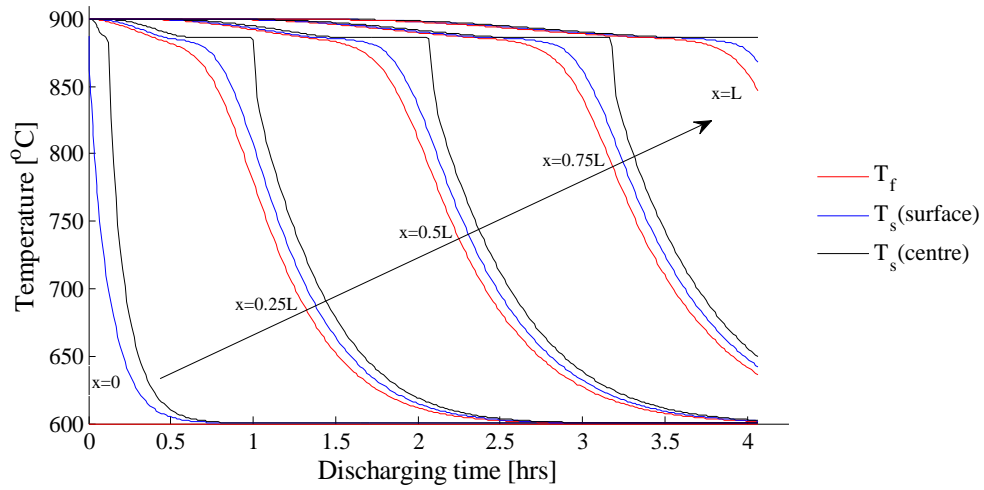


Fig. 5. Thermocline graph of 40 mm diameter macro-encapsulated Na_2SO_4 particles (61%wt Na_2SO_4 39%wt Al_2O_3).

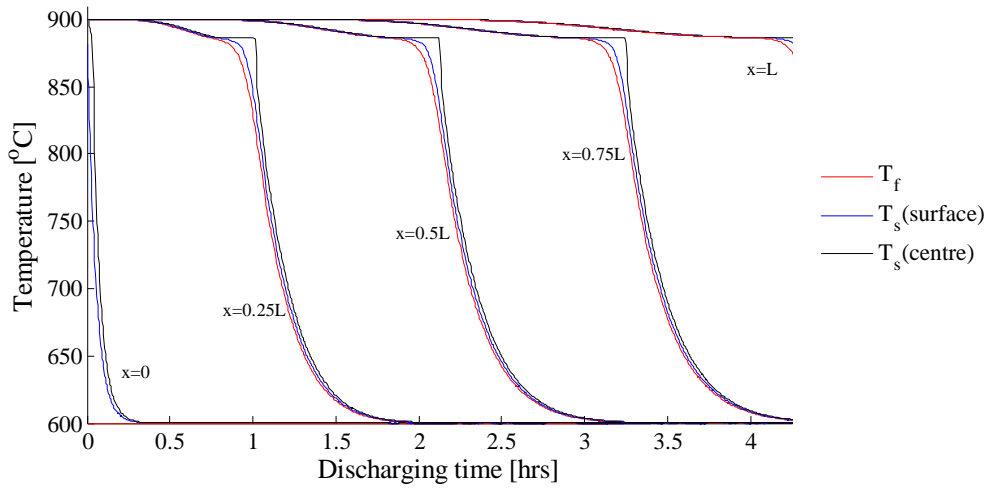


Fig. 6. Thermocline graph of 20 mm diameter macro-encapsulated Na_2SO_4 particles (61%wt Na_2SO_4 39%wt Al_2O_3).

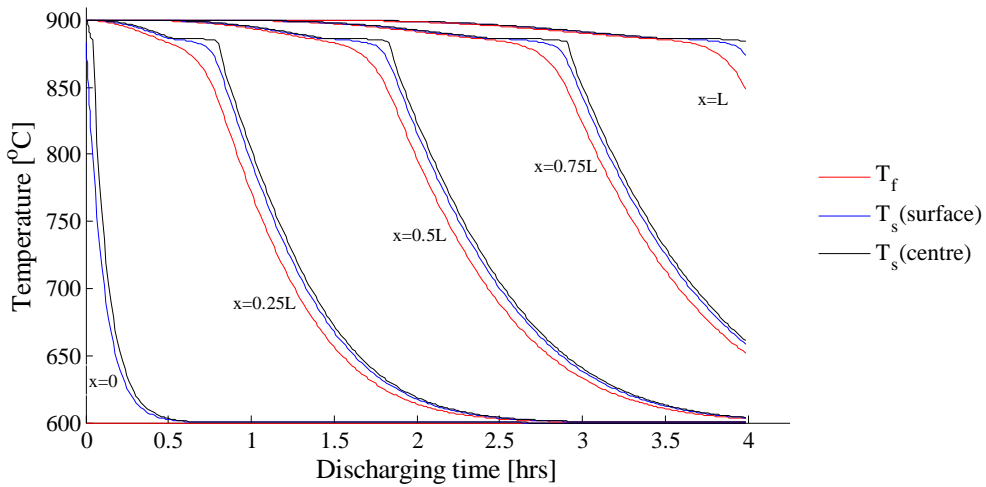


Fig. 7. Thermocline graph of 40 mm diameter micro-encapsulated Na_2SO_4 particles (36%wt Na_2SO_4 64%wt Al_2O_3).

The bulk thermal conductivity of the micro-encapsulated particles is increased by the alumina matrix, thus improving the intraparticle heat transfer. This is shown in Fig. 7 for the larger 40 mm diameter particles. A comparison with Fig. 5 reveals that the difference between the surface and centre temperatures of the micro-encapsulated particles is reduced. However, the gradient of the thermocline in Fig. 7 is not steeper than for the macro-encapsulated particles in Fig. 5. This indicates that the convective heat transfer in the packed bed is the dominant effect in generating a steep thermocline. Therefore internal rates of heat transfer are not the limiting factor in the efficiency of the storage (for the particle sizes analysed). Decreasing the particle diameter is the most effective mechanism to increase the storage discharge time for an EPCM packed bed.

5. Cost Analysis

Alumina spheres are commercially available from a number of suppliers. A price of R33/kg (excl. shipping) was quoted by the company Tipton Ceram Corporation for 20 tonnes of high alumina spheres (99.3-99.7 % purity). Sodium sulphate (99.7-100 % purity) can be sourced locally from the company CHC Resources at a cost of R2.65/kg excl. VAT (imported from Spain). The data presented in Table 2 indicates that the discharge time of the EPCMs is not significantly longer than solid alumina particles. Therefore in order for the EPCMs to be economically viable the cost of the material, including the encapsulation processing cost, should not exceed the cost of sensible heat storage in alumina. Based on this principle it is possible to estimate the maximum allowable encapsulation processing cost per pebble. This data is provided in Table 3.

Table 3. Estimate costs of packed bed filler materials for a 6 m³ packed bed

Material	Al ₂ O ₃ Cost *	Na ₂ SO ₄ Cost	Total Material Cost	Encapsulation Processing Cost Limit **	Encapsulation Cost Limit per 20 mm pebble ***	Encapsulation Cost Limit per 40 mm pebble ***
	[ZAR]	[ZAR]	[ZAR]	[ZAR]	[ZAR]	[ZAR]
Al ₂ O ₃	427 680	0	427 680	n/a	n/a	n/a
Na ₂ SO ₄ (Macro)	115 901	14 335	130 236	297 444	0.35	2.76
Na ₂ SO ₄ (Micro)	213 840	9 832	223 672	204 008	0.24	1.90

* assuming an alumina price of R33/kg for the EPCM and the pure alumina storage

** calculated by subtracting EPCM material cost from the cost of sensible heat storage in alumina (R427 680)

*** calculated by dividing encapsulation processing cost limit by the number of pebbles required to pack a 6m³ volume

The low encapsulation costs limits outlined in Table 3 show that an efficient automated processing method needs to be developed for this technology to be viable. Although the heat transfer in the 40 mm EPCM particles is inferior to the 20 mm particles (6-7 % decrease in discharge time), the higher encapsulation cost limit allows for a better manufacturing potential. In the near term the larger pebble size is considered optimal.

6. Conclusions and Future Work

A numerical model of the heat transfer in a packed bed of EPCMs was solved using orthogonal collocation on finite elements. The temperature profiles within macro and micro-encapsulated particles were studied for 20 mm and 40 mm particle diameters. The packed bed discharge times of the encapsulated Na₂SO₄ particles are similar to equivalent sized alumina particles, but the storage mass is reduced. The macro-encapsulated 20 mm diameter particles offer the best thermal storage performance. From a manufacturing perspective 40 mm diameter particles are likely to have the lowest encapsulating processing cost. The choice of macro or micro encapsulation method will depend strongly on the associated costs of the processing. Future work will involve developing a low cost processing technique to manufacture EPCMs of Na₂SO₄. Testing of such particles is scheduled to be completed by the end of 2014. The use of multiple PCMs with melting points between 600 °C and 900 °C will also be studied in order to increase the storage discharge time.

Nomenclature

Roman

a_p	Particle surface area to volume ratio [m^2/m^3]	t	Time [s]
c	Specific heat at constant pressure [J/kgK]	V	Volume [m^3]
D	Packed bed diameter [m]	U_x	Axial interstitial flow velocity [m/s]
d_p	Particle diameter [m]	x	Axial bed co-ordinate [m]
H	Specific enthalpy [J/kg]		
ΔH_{fs}	Enthalpy of fusion [J/kg]		
h_p	Convection heat transfer coefficient [$\text{W}/\text{m}^2\text{K}$]		
k	Thermal conductivity [W/mK]		
L	Bed Length [m]		
\dot{m}	Mass flow rate [kg/s]		
R	Particle radius [m]		
r	Radial particle co-ordinate [m]		
ΔT_m	Melting temperature range [K]		
T	Temperature [K]		

Greek

α	Thermal dispersion in fluid [W/mK]
ε	Packed bed void fraction
ρ	Density [kg/m^3]

Subscripts

f	Fluid phase
s	Solid phase
l	Liquid phase
eff	Effective property

References

- [1] T.H. Roos, N. Rubin, B.C. Meyers, M. Maliage, D. Dunn, S. Perumal and P. Klein. DPSS SPRP Progress Report for 2010/2011 and 2011/2012. SPRP-00000-00002-RPT, (2013).
- [2] L. Amsbeck, T. Denk, M. Ebert, C. Gertig, P. Heller, P. Herrmann, J. Jedamski, *et al.* Test of a Solar-Hybrid Microturbine System and Evaluation of Storage Deployment. Proceedings of the 16th SolarPACES Conference, Perpignan, France. (2010).
- [3] P. Klein, T.H. Roos, T.J Sheer. Experimental investigation into a packed bed thermal storage solution for solar gas turbine systems. Proceedings of the 19th SolarPACES Conference, Las Vegas, USA. (2013).
- [4] S. Too, R. Olivares, R. Benito, J. S. Kim, G. Duffy, and J. Edwards. High temperature thermal energy storage systems for open-cycle solar air Brayton plant. CSIRO publication EP12817 (2012)
- [5] W. Notter, T. Lechner, U. Groß, and E. Hahne. Thermophysical properties of the composite ceramic-salt system ($\text{SiO}_2/\text{Na}_2\text{SO}_4$). *Thermochimica acta* 218 (1993): 455-463.
- [6] T.D. Claar, and R.J. Petri. High-temperature direct-contact thermal energy storage using phase-change media. U.S. Patent 4,512,388, (1985).
- [7] J.F. Martin. Thermal energy storage technical progress report April 1985-March 1986. ORNL/TM-10247. (1987).
- [8] A. Mathur, R. Kasetty, J. Oxley, J. Mendez, K. Nithyanandam. Using encapsulated phase change salts for concentrated solar power plant. Proceedings of the 19th SolarPACES Conference, Las Vegas, USA. (2013).
- [9] Y. Goswami. Development of low cost industrially scalable PCM capsules for thermal energy storage in CSP plants. Sunshot presentation 2013.
- [10] N. Wakao, and S. Kaguei. Heat and mass transfer in packed beds (Vol. 1). Taylor & Francis US. (1982).
- [11] Z.X. Gong. Time-dependent melting and freezing of multiple phase change materials. PhD Thesis. McGill University. Canada. (1996).
- [12] O. Wilson, D. Groulx. Stefan's Problem: Validation of a One-Dimensional Solid-Liquid Phase Change Heat Transfer Process. Proceedings of the COMSOL conference, Boston, USA (2010).
- [13] I. Barin, O. Knacke, and O. Kubaschewski. Thermochemical properties of inorganic substances: supplement. Vol. 380. Berlin: Springer-Verlag, (1977).
- [14] G.J. Janz. Thermodynamic and Transport Properties of Molten Salts: Correlation Equations for Critically Evaluated Density, Surface Tension, Electrical Conductance, and Viscosity Data, *J. Phys. Chem. Ref. Data*, 17, Suppl. 2, (1988).